Travelling fire in full scale experimental building subjected to open ventilation conditions

Ali Nadjai
School Built Environment, University of Ulster, Newtownabbey, UK
Naveed Alam
FireSERT, University of Ulster at Jordanstown, Newtownabbey, UK
Marion Charlier
Department of Construction and Infrastructure Applications, Arcelormittal Global R&D, Esch-sur-Alzette, Luxembourg
Olivier Vassart
Steligence, ArcelorMittal Inc, Luxembourg, Luxembourg
Xu Dai
School of Engineering, University of Edinburgh, Edinburgh, UK
Jean-Marc Franssen
Universite de Liege, Liege, Belgium, and
Johan Sjostrom
RISE Research Institutes of Sweden AB, Mölndal, Sweden

Received 4 June 2021
Revised 18 March 2022
Accepted 20 April 2022

Abstract

Purpose – In the frame of the European RFCS TRAFIR project, three large compartment fire tests involving steel structure were conducted by Ulster University, aiming at understanding in which conditions a travelling fire develops, as well as how it behaves and impacts the surrounding structure.

Design/methodology/approach – During the experimental programme, the path and geometry of the travelling fire was studied and temperatures, heat fluxes and spread rates were measured. Influence of the travelling fire on the structural elements was also monitored during the travelling fire tests.

Findings – This paper provides details related to the influence of travelling fires on a central structural steel column.

Originality/value – The experimental data are presented in terms of the gas temperatures recorded in the test compartment near the column, as well as the temperatures recorded in the steel column at different levels. Because of the large data, only fire test one results are discussed in this paper.

Keywords Steel structure, Compartment fires, Travelling fires, Fire tests

Paper type Research paper

1. Introduction

The response of a structure subjected to fire is dependent on the fire exposure scenario. Small compartment fires behave in a relatively well understood manner, usually defined as a

This work was carried out in the frame of the TRAFIR project with funding from the Research Fund for Coal and Steel (grant No 754198). Partners are ArcelorMittal, Liège University, the University of Edinburgh, RISE Research Institutes of Sweden and the University of Ulster. The authors also wish to acknowledge the supporting of companies Sean Timoney & Sons Ltd, FP McCann Ltd, Saverfield Ltd and Crossfire Ltd.

Journal of Structural Fire Engineering
Vol. 14 No. 2, 2023
pp. 149-166

2040-2317
DOI 10.1108/JSFE-06-2021-0037

post-flashover fire, where the temperatures within the compartment are considered uniform. However, with modern architecture there is an important increase of open large-floor plan spaces, for which the assumption of post-flashover fire does not hold and there is instead a smaller localised fire that moves across the floor with time. The current design methods were developed using extrapolation of existing fire test data. These data come from small compartments tests for which a uniform distribution of gases and temperatures fit well. But as soon as large compartments are involved, this assumption does not hold anymore. After inspecting fires in large compartments that occurred during the past 2 decades, the conclusion is that such fires have a great deal of non-uniformity. They generally burn locally and move across the floor over time. This phenomenon generates non-uniform temperatures and transient heating of the structure. This type of fire scenario is currently idealized as travelling fires (Stern-Gottfried and Rein, 2012).

In the EN1991-1-2, 2002, only two models consider a non-uniform temperature distribution: the localised fire model and the advanced fire models (zone models and computational fluid dynamic models). Nevertheless, the localized fire method considers a static fire which do not translate the effect of a travelling fire. For zone models, the situation starts as a two-zones model based on the assumption of accumulation of combustion products in a layer beneath the ceiling, with a horizontal interface. Uniform characteristics of the gas may be assumed in each layer and the exchanges of mass, energy and chemical substance are calculated between these different zones. Although this model considers a non-uniform temperature distribution within the compartment, it does not translate the possible travelling nature of a fire. The CFD (computational fluid dynamic) models enable to solve numerically the partial differential equations giving in all points of the compartment, the thermo-dynamic and aero-dynamic variables. These models are consequently complex and imply a high computational cost.

Travelling fires have been observed in several structural failures especially from 2000: The World Trade Center Towers (Gann *et al.*, 2013) in New York City in 2001, the Windsor Tower (Fletcher *et al.*, 2005) in Madrid in 2005, and the Faculty of TU Delft Architecture building (Zannoni *et al.*, 2008) in Netherlands in 2008. The recent years have seen growing interest in investigating travelling fires which underlined the inadequacy of uniform heating in large compartments (Rein *et al.*, 2007; Horová *et al.*, 2013; Hidalgo *et al.*, 2017, 2019; Gamba *et al.*, 2020; Degler *et al.*, 2015; Charlier *et al.*, 2018; Rackauskaite *et al.*, 2015). Further research effort is still needed, especially to extend the experimental results of such fire scenarios.

2. Experimental programme

During the experimental programme, three large-scale fire tests were conducted in a compartment with different boundary conditions having similar fire load (Plate 1a). The floor plan between the outer gridlines of the test structure was 15 m × 9 m as shown in Figure 1. The level of the ceiling from the floor finish surface was 2.90 m. The test compartment is a representative of a modern office building and symbolizes a part of the entire office layout.

(a) (b) (c)

Plate 1.
Different opening layouts used for the three tests during the experimental programme, (a) Test 1: Opening area = 85.2 m^2, (b) Test 2: Opening area = 30 m^2, (c) Test 3: Opening area = 10 m^2

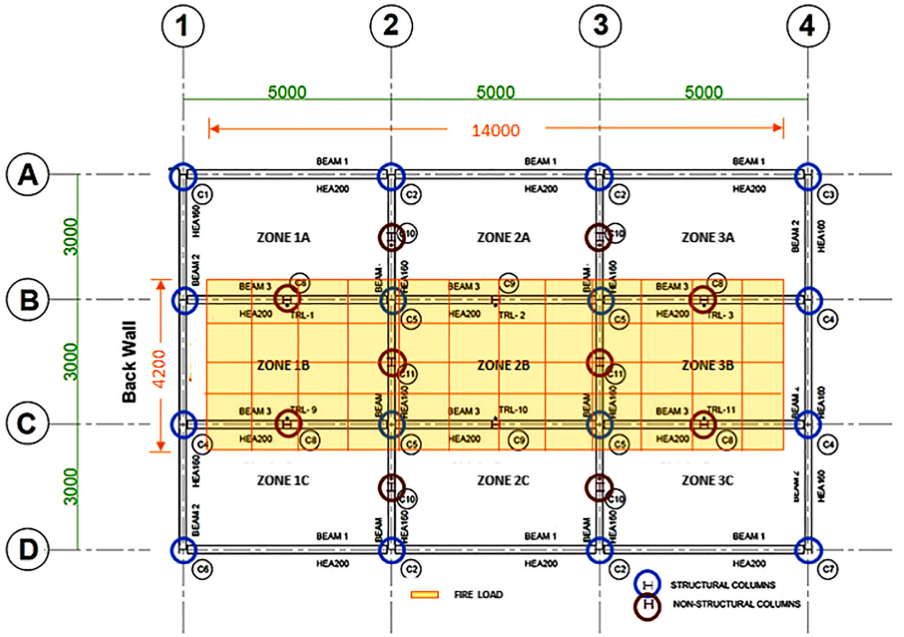

Figure 1.
Layout plan of the structure and location of the fuel load

The structure is made of steel beams and columns as the main structural frame while hollow-core precast slabs were used for the construction of roof. The layout of the structure on the ground was 15.2 by 9.2 m while the depth of the ceiling from the floor finish level was 2.90 m. The fire load used for the three tests is representative of an office building following references (EN1991-1-2, 2002; Gamba *et al.*, 2020).

2.1 Outline and formal structure

The structural steel frame of the test compartment was erected by Saverfield Ltd, local partner to FireSERT. The steel columns were separated into two categories, the structural columns and the dummy columns (see Plate 2). The structural columns were part of the steel frame transmitting the loads to the foundation while the dummy columns were not part of the structural steel frame and were only provided for data acquisition purposes.

All columns were fixed to the pre-existing reinforced concrete flooring via anchorage bolts. For the structural columns, four anchorage bolts were used while for the dummy columns, only two anchorage bolts were used for fixing purposes. The connections between the structural columns and beams were designed as fin-plates. The distance amongst the structural columns along the longer direction of the test compartment was 5,000 mm while the same along the shorter direction was 3,000 mm. The structural frame was laterally restrained using four diagonal bracings, two each along the longer and the shorter directions. The dummy columns provided for data acquisition purposes were anchored to the bottom flanges of the steel beams. The structural steel used for the construction of the test compartment was grade S355. Both the structural and dummy columns, as well as the beams provided along the longer direction, consisted for HEA 200 hot rolled steel sections (see Table 1). On the other hand, the beams in the shorter direction consisted of HEA 160 hot rolled steel sections. The roof consisted of 120 mm thick hollow-core precast concrete slabs spanning between the

beams along the shorter direction of the test compartment. Keeping in view the usage of the test compartment, the main structural columns of the steel frame were protected using intumescent coating to maintain the structural integrity during the three fire tests. It can be seen in Plate 2, that only the structural columns are protected while the dummy columns are kept unprotected for data acquisition purposes.

2.2 Details of the fire load

The fuel wood source consisted of the species "*Picea abies*" with an average density 470 kg/m^3 having a moisture content of 15.22%. As the test compartment was a representative of an office building, the Eurocodes provide a medium fire growth rate ($t_\alpha = 300$ s) and a fire load density of 511 MJ/m^2 for such occupancy. In the frame of TRAFIR RFCS project, Gamba *et al.* (2020) performed a series of fire tests with uniformly distributed cellulosic fire loads making an arrangement which was a representative of an office building according to Eurocode 1. This work led to devise a well-established methodology, used to define the fuel load for the experimental campaign described in this paper. To achieve a medium fire growth rate for the office building, 9 layers of wooden sticks with an axis distance of 120 mm (90 mm intervals) were provided in three different directions. The wood sticks were 30 mm wide and 35 mm deep. The first layer of the wooden sticks was laid at 60° angle while the second was laid at an angle of 120°. The third layer was at 0° or 180° and the process was repeated in such a way the 6th layer of the sticks laid at 0° or 180° had a lateral offset of 60 mm with respect to the third layer as shown in Plate 2. The final layer, the ninth layer of the fuel wood was at 0° or 180°, such an arrangement helped to visually observe the travelling behaviour of fire from one wood stick to another. The fuel load arrangement was kept the same during all three tests while the boundary conditions were varied from one test to another as shown earlier in Plate 1.

The fuel wood was provided along the centre of the test compartment, as shown in Plate 3. The fire load was 14 m long stretching from wall to wall along the longer dimension of the test compartment. For convenience, a gap of 500 mm was maintained between the walls and the edge of the fuel bed at both ends. The width of the fuel bed was 4.2 m and was aligned with the centre line of the compartment. Such an arrangement of the fire load resulted in 2.4 m distance from the edge of the fuel bed to the centreline of the columns provided along in the longer

(a) (b)

Plate 2.
Fuel load arrangement and steel columns, (a) protected and unprotected columns with fuel weed, (b) a closer view of the fuel wood used during the experimental programme

Description	Sections	Section Factor (m^{-1})	Length Height (m)	Protection applied
Structural columns	HEA 200	209.5	3.5	Yes: R60
Dummy columns	HEA 200	209.5	2.7	No
Long beams	HEA 200	172.3	4.8	No
Short beams	HEA 160	138.0	3.0	No

Table 1.
Description of the steel structure

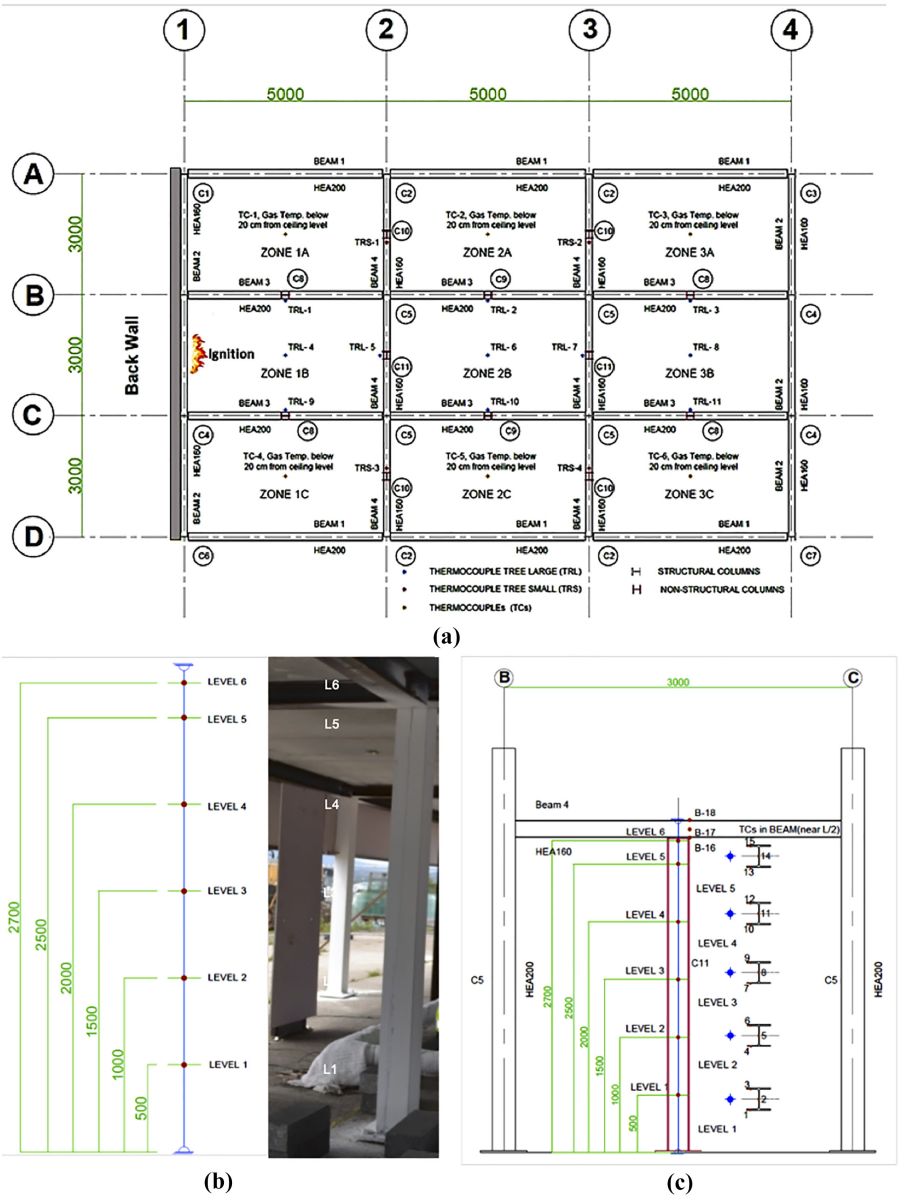

Plate 3.
Location of the thermocouple trees in the test compartment and detail of thermocouples for the central zone (a) positioning of thermocouple trees, (b) details of thermocouple trees, (c) detail of column thermocouples

dimension along gridline A and D. The fuel wood sticks were provided on a platform constructed using concrete blocks and gypsum fireboards as shown in Plate 2. The top surface of the platform was at a 325 mm height from the floor finish level.

3. Details of the instrumentation

The purpose of these large-scale tests was to investigate the dynamics of the travelling fires and to record fire related data. The recorded data included the compartment temperatures,

temperatures in the structural steel components, the heat fluxes, and the mass loss of the fuel wood. For the data acquisition, intensive instrumentation was applied, which consisted of thermocouples, heat flux gauges, thin-skinned calorimeters, anemometer, and the load cells (see detail of the large thermocouple trees, placed in the centreline of the compartment, in Plate 3, labelled TRL-1 to TRL-11).

In addition to the data recorded in the compartment, temperatures were also recorded in the steel frame during the tests. Temperatures in the steel frame were recorded in the non-structural columns (see Plate 3) and the selected beams. All thermocouples were provided at 3 mm depth from the surface of the flanges and the steel web. The heat fluxes were monitored via Gordon Gauges (GGs) and the thin-skinned calorimeters (TSCs).

3.1 Mass loss recording

The mass loss was monitored in the middle of the test compartment between gridlines 2 and 3 using a steel platform as shown in Plate 4. The steel platform was 3 m long × 5 m wide and was supported using four load cells a shown in Plate 4. To avoid any damage to the platform during the fire tests, fire blanked was wrapped around the steel elements. The load cells were also protected using the fire blanket to avoid any damage resulting from rise in temperatures. On top of the steel platform, two layers of gypsum fire board were provided to support 4.2 × 3.6 m of the fuel wood. The layers of the fire board were placed 325 mm from the floor finish level and were aligned with other fire board panels used to support the fuel wood. Although the fire boards supporting the fuel wood above the steel platform were at the same level, these were kept segregated from the rest of the floorboards to ensure separation of the fuel wood for accurate measurement of the mass loss during the fire tests.

3.2 Data logging system

All the assigned sensors were connected to the data logging system (calibrated and checked before use) through extension cables. The extension cables were stretched along the roof and were connected with the data loggers stationed in the site office as shown in Plate 6. A layer of fire blanket was laid under these cables to evade any damage from the heat during the tests. Due to higher number of sensors applied, multiple data loggers were employed during the tests. All data loggers were started earlier and began recording the data a few minutes before the start of the test. The early start times for each data logger were noted and later subtracted from the final recorded data to ensure uniformity of the data and to ensure data synchronization.

4. Results and discussion

In this paper only the first fire test results are presented. Plate 6 illustrates the travelling fire taking place along the length of the compartment through photographs and graphs plotting the evolution of gas temperatures in the compartment along the longer dimension, parallel to the path of the travelling fire. This is represented via five thermocouple trees (TRL-4 to TRL-8) equipped with six sensors each as shown earlier in Plate 3. The first thermocouple tree was positioned in the middle of zone 1 B at 1.5 m from the source of ignition. The remaining thermocouple trees (TRL-5 through TRL-8) along the centreline of the compartment were equidistant and positioned at 2,500 mm centres.

The maximum temperatures recorded at TRL4 were more than 1000 °C after 20 min from ignition but were measured for a very limited period, the gas temperatures quickly decreased to reach the interval [800–900 °C]. It is interesting to note that the plateau of the maximum recorded temperatures is longer at upper levels as compared to the lower levels. With the fire band travelling towards the next thermocouple tree, TRL5, the temperatures recorded at

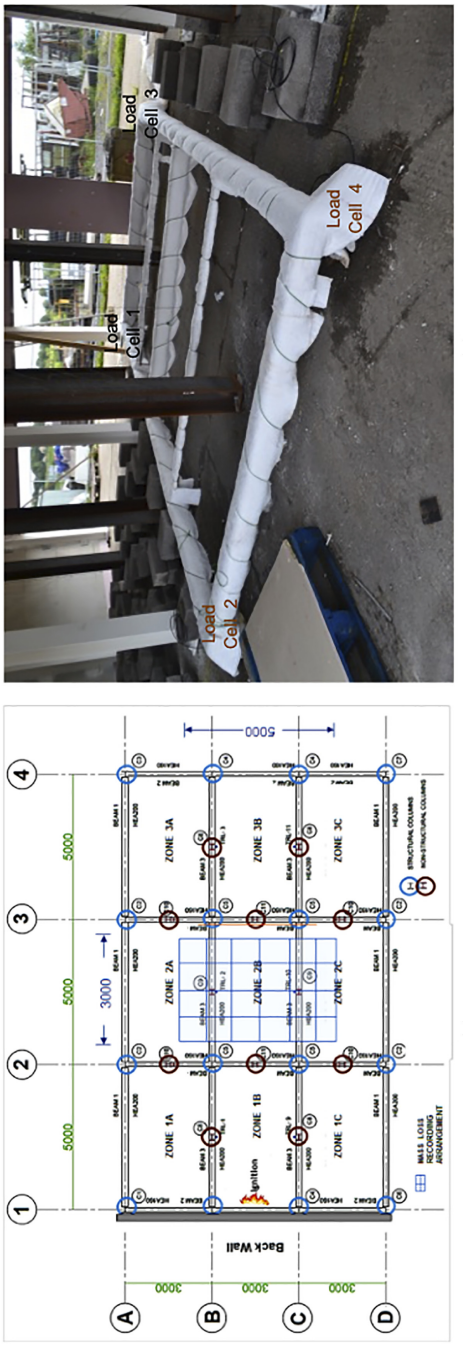

Plate 4.
Position and arrangement of the mass loss recording though four load cells, (a) location of steel platform to record mass-loss, (b) steel platform with load cells

TRL4 reduced while the temperatures at TRL5 increase. Temperatures recorded at TRL-5 reached the 900 °C after 38 min from the ignition. Similarly, the maximum recorded temperatures using TRL6, TRT7 and TRT8 at level 2 were 995 °C, 975 and 1,000 °C after 50 min, 57 min and 70 min from ignition respectively as shown in Plate 6. It is quite clear that the recorded temperatures vary along the height of the compartment, and that the TRL6 to TRL8 (placed in the second half of the compartment) present a shorter temperature peak as compared to TRL4 and TRL5 (placed close to the ignition) for 2 m height from floor finish level.

4.1 Experimental observation of the ravelling fire

Figure 2 demonstrates the experimental fire test starting from a single ignition point and developing into a travelling fire of a duration of 1 h and 20 min until all fuel is consumed. The initial fire spread was in all directions making a circle around the point of ignition. After 16 min from ignition, the length of the fire band was approximately 2 m while the growth of the fire was in the shape of a semi-circle or a curve.

At 28 min the fire initiated its travel from the backend of the compartment towards the fore-end along the fuel bed. At 23 min the difference between the lengths of fire band along the middle of the fuel bed was significantly higher as compared to that along the outer edges.

Burning of the fuel wood, supported by the platform provided to record the mass loss, started after 37 min from ignition. After 49.5 min from ignition, the centre of the travelling fire band reached the middle of the test compartment, zone 2 B. It was also observed that the fore-end of the travelling fire band had reached the last the end of the platform used to measure the mass loss. After 64 min from ignition, the fuel on the steel platform provided to measure the mass loss was mostly consumed. After 76 min from the start of the test, the intensity of the fire reduced significantly with the consumption of fuel wood. The flame size reduced as the far-end of the fuel wood kept burning. This burning of the fuel wood continued for a few more minutes. After 81 min from ignition, the fuel wood was consumed, and no flames were visible in any part of the test compartment. The data recording continued for further 39 more minutes, which provided a data set of 120 min altogether.

The maximum flame thickness (i.e. length of the fire along the longer dimension of the compartment) was observed during the test and is presented in Figure 3. The square markers correspond to a translation of the observations during the test, while the triangle markers correspond to inspection made from the video recording. The travelling behaviour of the fire (i.e. when the back end of the fire begins to travel) starts at 28 min from ignition for test no 1. This evolution suggests a fairly constant flame thickness of around 3.5 meters, with the lowest value occurring when the fire reaches the central bay of the compartment.

In addition to the temperatures recorded using the thermocouple trees, temperatures in the compartment at the ceiling level were monitored using individual thermocouples. The recorded temperatures at ceiling level in zone B along the centre of the compartment are given in Figure 4. The temperatures in zone 1B reach the maximum values after 23 min from ignition and gradually reduce with the fire travelling towards the fore-end of the compartment.

Plate 5.
Extension cables for data sensors and data loggers

(a)

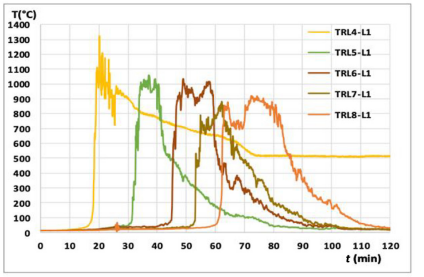

(b)

(c)

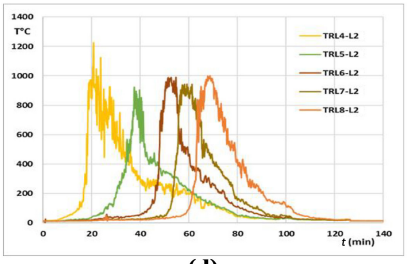

(d)

(e)

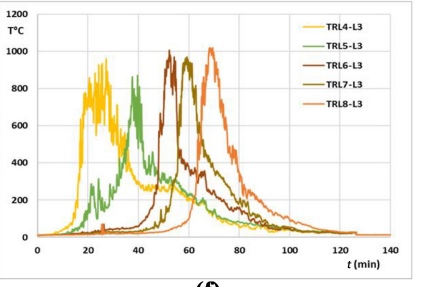

(f)

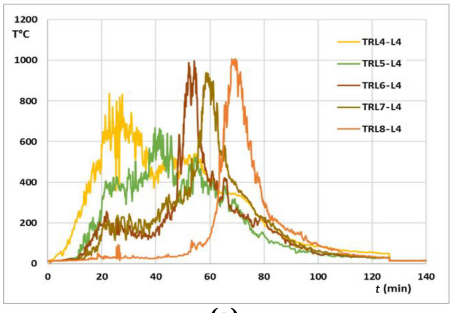

(g)

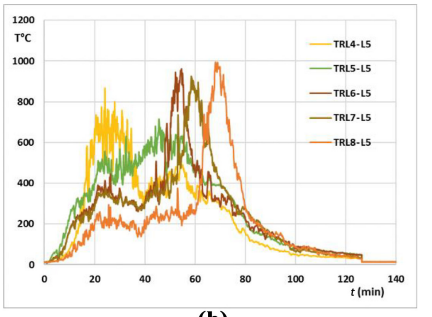

(h)

Plate 6.
Photographs of the fire and evolution of gas temperatures measured in TRL-4 to TRL-8 at 5 different levels, (a) photo after 12 min, (b) data at 0.5 m height, (c) photo after 30 min, (d) data at 1.0 m height, (e) photo after 45 min, (f) data at 1.5 m height, (g) data at 2.0 m height, (h) data at 2.5 m height

The recorded temperatures in the centre of the compartment in zone 2B are 950 °C after 50 min from ignition while these are 980 °C after 70 min of ignition for zone 3B. In all cases, a gradual increase in temperatures is observed which reduces as the fire travels ahead.

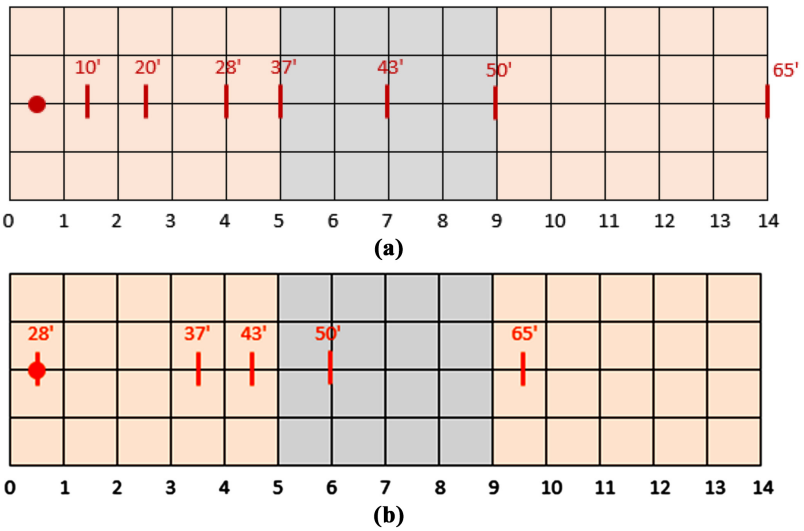

Figure 2.
Evolution of the maximum flame thickness, (a) evolution of the front, (b) evolution of the burnout

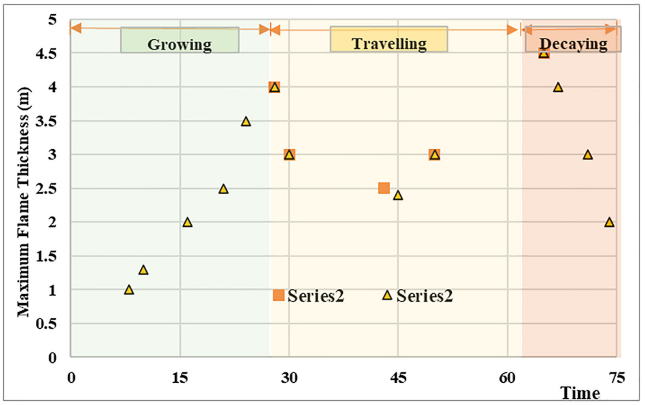

Figure 3.
Evolution of the maximum flame thickness

4.2 Results of temperatures in the steel structure

Temperatures were recorded in the selected beams and the unprotected dummy columns. In this paper the column and beam along gridline 3 positioned between gridlines B and C have been selected for data presentation purposes as shown in Plate 4. During the test, it was observed that the fore-end of the travelling fire reached the fuel wood beneath the selected beam after 52 min from ignition. Temperatures recorded in the compartment adjacent to the selected column using thermocouple tree TRL-7 are presented in Figure 5. The temperature rises at higher levels L5 and L6 initiates earlier as compared to that at the lower levels. The temperature rise at L4 is earlier as compared to the remaining lower levels while it is slower in comparison with levels L5 and L6. This could be explained by the hot gases rising in the compartment, establishing in the upper part. For the bottom three levels, the increase in temperature is rapid as temperatures rise from 100 °C to 950 °C within a few minutes, translating the direct contact with the flames.

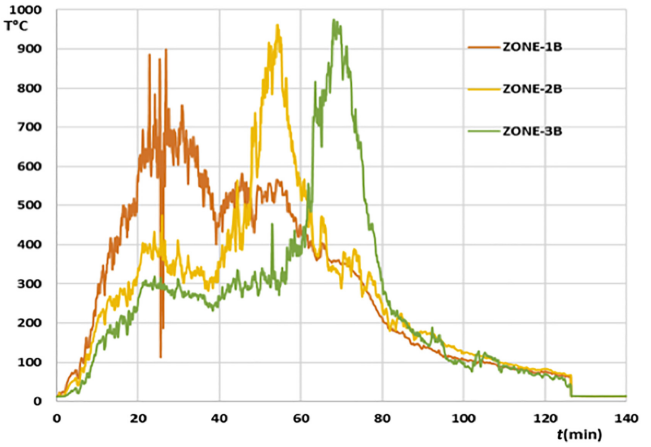

Figure 4.
Recorded temperatures at the ceiling level along the centre of the compartment (zone B)

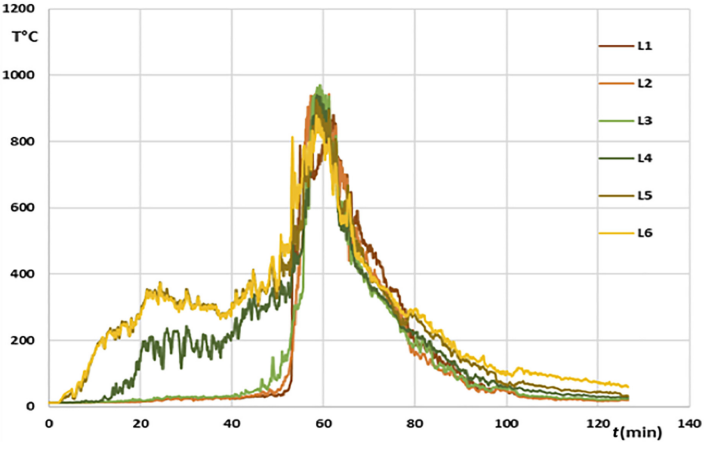

Figure 5.
Recorded gas temperatures in the thermocouple tree near the selected column and beam – TRL-7

The temperatures recorded in the flanges and the web of the column at level 3 are presented in Figure 6. Temperatures at level 2 rise after 52 min from ignition while those at level 4 rise after 15 min. For the first 50 min from ignition, the rise in temperature at level 4 is slow while it rises significantly as the fuel wood near the column starts to burn. The temperatures recorded across the section of the column at each level can be considered as uniform.

The label "LHS-F" corresponds to the flange closer to gridline C (i.e. those with thermocouple numbers 1, 4, 7, 10, 13 in Plate 3), "WEB" corresponds to the web and "RHS-F" corresponds to the flanges closer to gridline B (i.e. those with thermocouple numbers 3, 6, 9, 12, 15 in Plate 3). It can be seen that the temperature profiles in steel are similar to the gas temperature profiles recorded in the compartment, with the following differences:

(1) The maximum steel temperature is 803 °C at 63 min (versus 937 °C at 58 min for gas temperature): this decrease, and delay translate the effect of the steel thermal inertia.

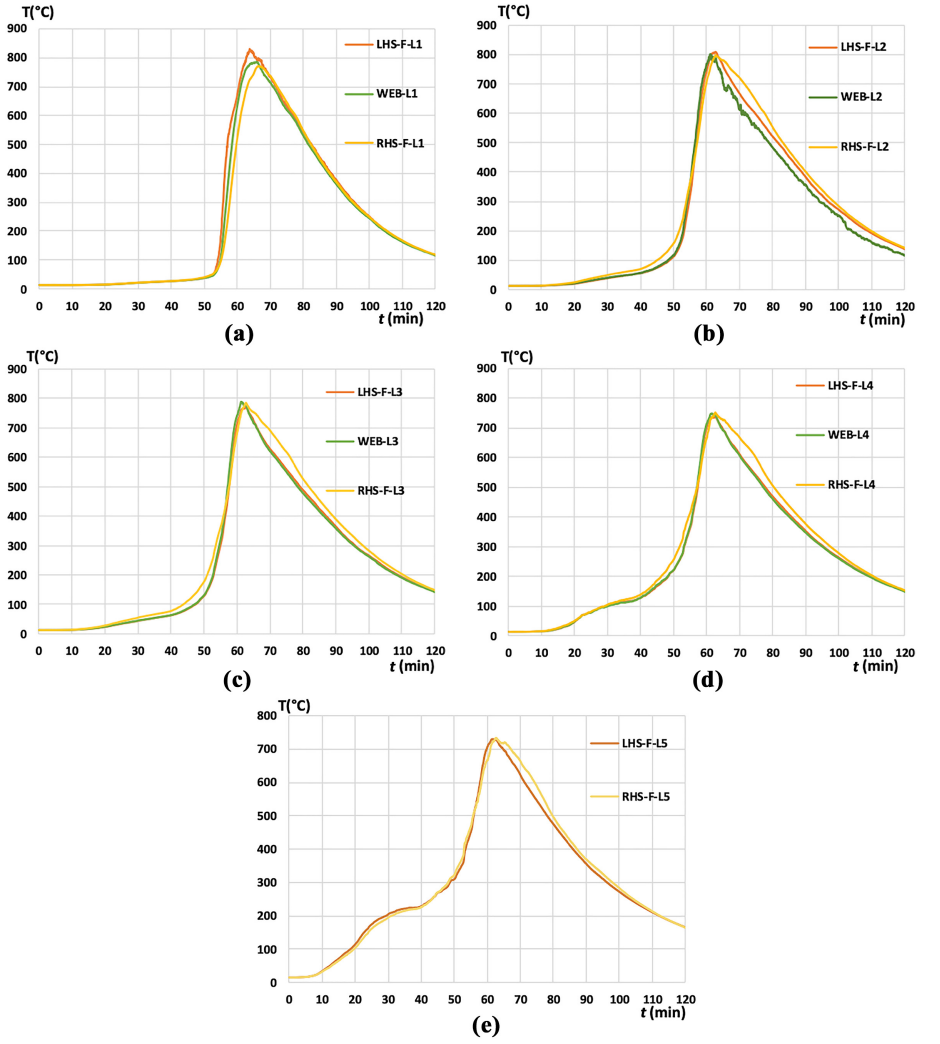

Figure 6.
Steel temperatures at different locations along the height of the column, (a) 0.5 m height, (b) 1.0 m height, (c) 1.5 m height, (d) 2.0 m height, (e) 2.5 m height

(2) The steel temperature descending branch is less steep than the gas temperature one (it reaches 500 °C after around 80 min while the gas temperature one reaches this value after around 67 min).

(3) Also, the temperatures recorded across the section of the column at each level can be considered as uniform.

4.3 Mass loss of the burning fuel

The mass loss data recorded during the test is presented in Figure 7. As observed during the test, a decrease in the mass of the fuel wood supported on the platform is seen once it catches fire after 37 min from ignition. After 39 min, a uniform decrease in the wooden fuel mass is recorded. After 58 min from ignition, a slow reduction in the mass loss is recorded due to

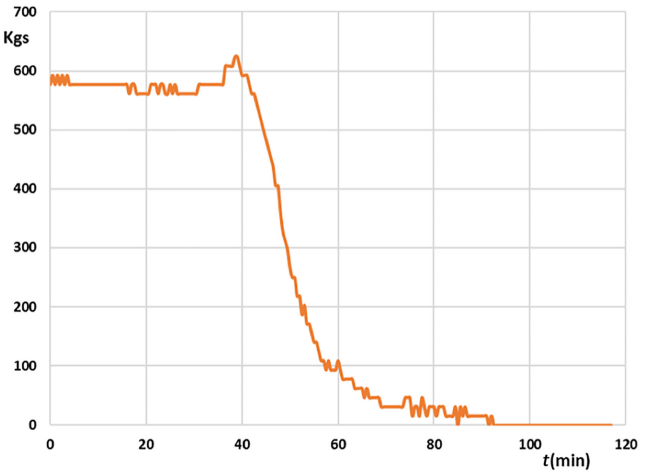

Figure 7.
Recorded mass loss

non-uniformity of the burning fuel. The mass loss recordings also comply with the observations made during the test where most of the fuel wood provided on the platform was consumed after 64 min recoded in the selected column next to TRL7. At 37 min, an increase in the fuel mass is recorded which is physical impossible and non-realistic. Such odd values are result of the vibrations caused by the approaching fire when it interferes with the fuel mass supported by the platform resting on load cells. The load cells being very sensitive record such variations due to vibrations caused by the approaching fire. Similar variations have been previously reported by Gamba *et al.* (2020) during their experimental program as well.

The mass loss rate [kg/s] is the variation of the solid fuel mass during the combustion process. It is possible to deduce the rate of heat release (RHR) from the mass loss rate, since these two parameters are linked by equations (1) and (2), H_u being the net calorific value [MJ/kg] and m being the combustion factor (considered equal to 0.8). To evaluate the mass loss rate from the continuously measured mass, a backward finite difference scheme must be applied, which requires the definition of a fixed time step. There is no unique correct value for this time step; but the following consequences should be considered: a more important time step implies a smoother curve, while a less important time step translates the measurements in a more precise way but might provide unrealistic peaks (noise and outliers). Finally, a time step $\Delta t = 60$ s was considered as an acceptable compromise.

$$RHR(t) = H_u.m.MLR(t) \tag{1}$$

$$RHR(t) = -H_u.m.\frac{dm}{dt} = -H_u.m.\frac{\Delta m}{\Delta t} \tag{2}$$

As the mass loss rate is the derivative of an experimental signal, noise and outliers (for example, negative values) are quickly generated. One method to cope with this is to filter the curve using, for example, a Savitzky–Golay filter. This digital filter that can be applied to a set of digital data points for the purpose of smoothing the data, that is, to increase the precision of the data without distorting the signal tendency. This is achieved, in a process known as convolution, by fitting successive sub-sets of adjacent data points with a low-degree polynomial. The simplest form of this approach, called running average, consists in computing the average for each subset. This approach is commonly used with time series data to smooth out short-term fluctuations and highlight longer-term trends or cycles.

The RHR [kW] obtained by derivative of the mass loss using a time step of 60 s, the filtered RHR obtained with smoothing parameters of 10 and 20 are depicted in Figure 8. The filtered RHR with parameters 10 and 20 show maxima values of 8,140 kW and 5,850 kW, respectively. It also has to be noted that some discrepancies can be noticed with wooden fuel load, at the end of the combustion process. Indeed, the heat of combustion of wood is not perfectly constant: it is higher at the end of a test when only embers are left.

5. CFD simulations

Several CFD simulations were launched with FDS software to calibrate the model representing the large-scale tests. These CFD simulations consider a simplified representation of the continuous fire load consisting of discrete volumes based on a regular arrangement (Charlier *et al.*, 2021). The proposed approach can allow for both an acceptable representation of the travelling fire in terms of fire spread and steel temperatures while being less computationally demanding than modelling the exact geometry of the fire load, making it more desirable for practical applications.

In a first simplified step, the CFD output "THERMOCOUPLE" was used to evaluate the related steel temperature using the incremental formula from EN1993-1-2 section 4.2.5.1 providing the increase of temperature $\Delta\theta_{s,\Delta t}$ in an unprotected steel member during a time interval Δt, see equation (3) (CEN (European Committee for Standardization), 2005). These results accommodate the radiation effect, which is evaluated from all direction as the thermocouple is modelled as a sphere. They also consider the convective exchange with environment gas. For each time step, $\dot{h}_{net,t}$ (net heat flux per unit area) is determined whilst computing the net convective and radiative fluxes. This method considers a constant temperature through the section for a given height.

$$\Delta\theta_{s,\Delta t} = k_{sh}\frac{\frac{A_m}{V}}{C_s\rho_s}\dot{h}_{net,t}\Delta t \tag{3}$$

Where

k_{sh} is the correction factor for the shadow effect [–];

A_m/V is the section factor for unprotected steel elements [1/m];

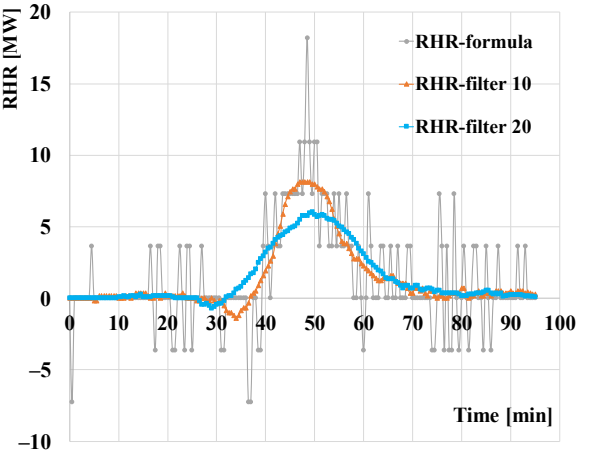

Figure 8.
Approximation of the RHR derived from the mass loss measurements

A_m is the surface area of the member per unit length [m^2/m];
V is the volume of the member per unit length [m^3/m];
c_s it is the specific heat of steel [J/kg K];
$\dot{h}_{net,t}$ is the value of the net heat flux per unit area [W/m^2];
Δt is the time interval [s]; and
ρ_s is the unit mass of steel [kg/m^3].

In a second and more complex step, a coupling between CFD (FDS software) and FE (SAFIR® software version 2019b0 (Franssen and Gernay, 2017)) was used. Radiative intensities and gas temperatures calculated by FDS have been used by SAFIR® to calculate the temperatures in the steel column. Figure 9 provides the evolution of the steel temperatures across the section located at Level 3, as a function of time and at five points of interest (also highlighted on Figure 9). From the start of the fire until around 40 min: steel temperatures are below 100 °C, and all five curves follow a similar evolution. Steel temperatures then slowly start to increase for the next twenty minutes to reach approximately 200 °C. The point 3 (located in the web which is the thinner part of the section) heats up quicker, followed by the points 2 and 5 as these points corresponds to the left part of the profile (facing gridline 1). A fairly sharp increase in temperatures is met at around 60 min and the maximum steel temperatures are met at around 70 min, for a quite short period of time. Indeed, temperatures start to drop from around 70 min until around 90 min (where they reach around 200 °C). During the decay phase, points 2 and 5 cool slightly faster, in accordance with the relative position between the profile and the fire. Nevertheless, the steel temperatures at the five points of interest present globally a similar evolution. As the temperature gradient within the section being quite limited (and the same tendency is observed for the different levels of the column), it allows to then present the evolution of the steel temperatures resulting from the SAFIR analysis as the average of the steel temperatures from the five points of interest.

As explained previously, steel temperatures were recorded at five different levels on unprotected columns placed in the centerline of the compartment, with three thermocouples provided at each level such that one is positioned in the web while the others are positioned in the flanges. The numerical results (are compared with the steel temperatures which were recorded at five different levels in the column next to TRL-7. The comparison of the results is encouraging as it is shown in Figure 10 for level 3. Further information is provided in Charlier *et al.* (2018). The details related to the second fire test can be found in reference (Alam *et al.*, 2022) of this article.

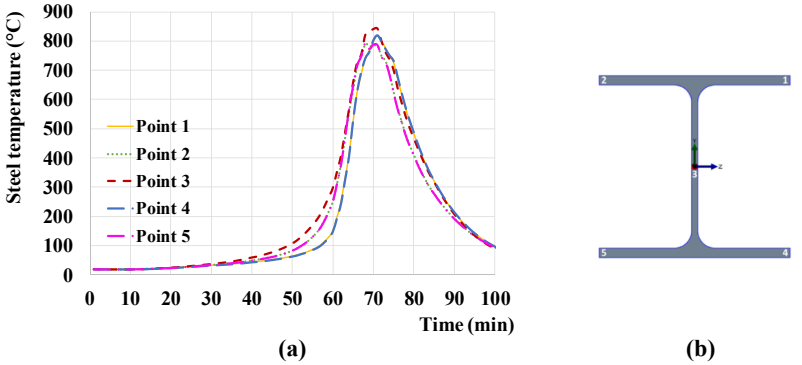

Figure 9.
(a) Steel temperatures evolution at Level 3 from SAFIR at different locations of the section for the test *n*°1., (b) selected thermocouple positions

6. Conclusions

Three large scale tests were performed in real building dimensions to represent the travelling fire as realistic as possible; however, only one test fire results are presented in this paper, and this is due to the recorded large data. Instrumentation was installed to measure atmospheric temperatures, surface temperatures, heat fluxes and temperature within the steel columns, beams and boundaries conditions of the surrounding compartment. In this paper only of the first of the three conducted tests is described and the evolution of the following results were presented: gas temperatures recorded in the central part of the compartment, along its length, maximum flame thickness, steel temperatures in a central beam and a central column, as well as mass loss data. Following are major conclusions from the travelling fire experimental test 1.

(1) For the fire initiating at a single point, its developing phase consists of increase in the volume of fire in all directions making a circle around the point of ignition. Once the fire is well developed, it continues to travel along the fuel bed. In the case of the test conducted during this research, the fire travelled in the forward direction towards the fore end of the compartment. However, the fire could travel in any direction depending upon the availability of the fuel.

(2) The temperatures in the compartment were found to be dependent on the positioning of the travelling fire. The parts of the compartment around the fire are hotter while the parts away from the fire were at lower temperatures.

(3) The results obtained from the fire test demonstrated the non-uniform temperature distribution, leading to the heating of the nearby structural steel elements, resulting in a reduction of individual members' resistance, which could influence the global structural stability.

(4) The walls and precast slabs forming the boundary of the compartment retained its integrity despite a significant thermal gradient across the wall and slabs. In addition, all the connections and steel members performed very well and showed no signs of failure during the three conducted fire tests.

(5) The results obtained from the CFD modelling were quite similar to those obtained during the test with the main difference being the maximum temperatures. The steel

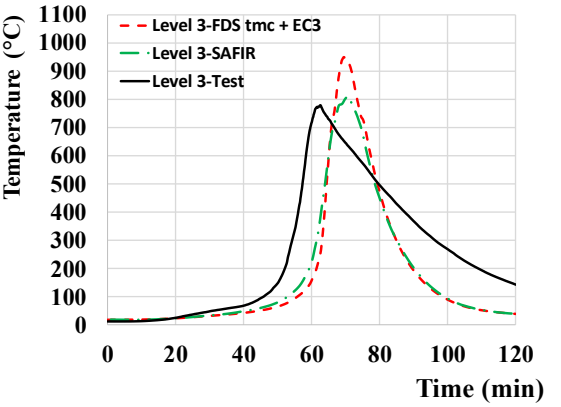

Figure 10.
Comparison of the experimental and numerical steel temperatures in a central column at level 3 (i.e. at 1.5 m height)

temperatures obtained via CFD modelling generally displayed a good agreement with the test but underestimated the descending branch.

References

Alam, N., Ali, N., Charlier, M., Vassart, O., Welch, S., Sjöström, J. and Xu, D. (2022), "Large scale travelling fire tests with open ventilation conditions and their effect on the surrounding steel structure– the second fire test", *Journal of Constructional Steel Research*, Vol. 188, 107032, doi: 10.1016/j.jcsr.2021.107032, ISSN 0143-974X.

CEN (European Committee for Standardization) (2005), *EN 1993-1-2: Eurocode 3: Design of Steel Structures - Part 1-2: General Rules - Structural Fire Design*, Brussels.

Charlier, M., Gamba, A., Dai, X., Welch, S., Vassart, O. and Franssen, J.M. (2018), "CFD analyses used to evaluate the influence of compartment geometry on the possibility of development of a travelling fire", *Proceedings of the 10th International Conference on Structures in Fire (Ulster University)*, Belfast, UK, pp. 341-348.

Charlier, M., Glorieux, A., Dai, X., Alam, N., Welch, S., Anderson, J., Vassart, O. and Nadjai, A. (2021), "Travelling fire experiments in steel-framed structure: numerical investigations with CFD and FEM", *Journal of Structural Fire Engineering*.

Degler, J., Eliasson, A., Anderson, A., Lange, D. and Rush, D. (2015), "A- priori modelling of the Tisova fire test as input to the experimental work", *Proceedings of the first International Conference on Structuraa, Safety under Fire and Blast*, Glasgow, UK.

EN1991-1-2 (2002), *Eurocode 1: Actions on Structures – Part 1-2: General Actions on Structures Exposed to Fire*, CEN, Brussels.

Fletcher, I., Borg, A., Hitchen, N. and Welch, S. (2005), "Performance of concrete in fire: a review of the state of the art, with a case study of the Windsor Tower fire", in *4th International Work- Shop in Structures in Fire*, pp. 779-790.

Franssen, J.-M. and Gernay, T. (2017), "Modeling structures in fire with SAFIR®: theoretical background and capabilities", *Journal of Structural Fire Engineering*, Vol. 8 No. 3, pp. 300-323, doi: 10.1108/JSFE-07-2016-0010.

Gamba, A., Charlier, M. and Franssen, J.M. (2020), "Propagation tests with uniformly distributed cellulosic fire load", *Fire Safety Journal*, Vol. 117, 103213.

Gann, R.G., Haminutes, A., McGrattan, K., Nelson, H.E., Ohlemiller, T.J., Prasad, K.R. and Pitts, W.M. (2013), "Reconstruction of the fires and thermal environment in World Trade Center buildings 1, 2, and 7", *Fire Technology*, Vol. 49, pp. 679-707.

Hidalgo, J.P., Cowlard, A., Abecassis-Empis, C., Maluk, C., Maj- dalani, A.H., Kahrmann, S., Hilditch, R., Krajcovic, M. and Torero, J.L. (2017), "An experimental study of full-scale open floor plan enclosure fires", *Fire Safety Journal*, Vol. 89, pp. 22-40.

Hidalgo, J.P., Goode, T., Gupta, V., Cowlard, A., Abecassis-Empis, C., Maclean, J., Barlett, A., Maluk, C., Montalva, J.M., Osorio, A.F. and Torero, J.L. (2019), "The Malveira fire test: full-scale demonstration of fire modes in open-plan compartments", *Fire Safety Journal*, Vol. 108, 102827.

Horová, K., Jána, T. and Wald, F. (2013), "Temperature heterogeneity during travelling fire on experimental building", *Advances in Engineering Software*, Vols 62-63, pp. 119-130.

Rackauskaite, E., Hamel, C., Law, A. and Rein, G. (2015), "Improved formulation of travelling fires and application to concrete and steel structures", *Structures*, Vol. 3, pp. 250-260.

Rein, G., Zhang, X., Williams, P., Hume, B., Heise, A., Jowsey, A., Lane, B. and Torero, J.L. (2007), "Multi-storey fire analysis for high- rise buildings", *Proceedings of the 11th International Interflam Conference*, London, UK, pp. 605-616.

Stern-Gottfried, J. and Rein, G. (2012), "Travelling fires for structural design – Part I: literature review", *Fire Safety Journal*, Vol. 54, pp. 74-85.

Zannoni, D.M., Bos, J.G.H., Engel, D.K.E. and P. dr., U. (2008), *Brand Bij Bouwkunde*, Rosenthal.

Corresponding author
Ali Nadjai can be contacted at: a.nadjai@ulster.ac.uk